

Published in final edited form as:

Cell Rep. 2013 August 29; 4(4): 625–632. doi:10.1016/j.celrep.2013.07.036.

Grk5l Controls Heart Development by Limiting mTOR Signaling During Symmetry Breaking

Martin D. Burkhalter¹, Gregory B. Fralish², Richard T. Premont³, Marc G. Caron^{2,3,4}, and Melanie Philipp⁵

¹Leibniz Institute for Age Research, Fritz Lippmann Institute, 07745 Jena, Germany

²Department of Cell Biology, Duke University Medical Center, Durham, NC, 27710, USA

³Department of Medicine, Duke University Medical Center, Durham, NC, 27710, USA

⁴Department of Neurobiology, Duke University Medical Center, Durham, NC, 27710, USA

⁵Department of Biochemistry and Molecular Biology, Ulm University, 89081 Ulm, Germany

Abstract

The correct asymmetric placement of inner organs is termed situs solitus and is determined early during development. Failure in symmetry breaking results in conditions ranging from randomized organ arrangement to a complete mirror image, often accompanied by severe congenital heart defects (CHD). We found that the zebrafish homolog of mammalian G protein-coupled receptor kinase 5 (GRK5) employs non-canonical, receptor-independent functions to secure symmetry breaking. Knockdown of GRK5's closest homolog in zebrafish embryos, Grk5l, is sufficient to randomize cardiac looping and left-right asymmetry. Mechanistically, we found that loss of GRK5 increases mTORC1 activity. This causes elongation of motile cilia in the organ of laterality, a consequence known to be sufficient to trigger false organ arrangement. By fine-tuning mTORC1, GRK5 thus has an unanticipated function during early development, besides its well-characterized role in the adult heart. These findings thus could implicate GRK5 as a susceptibility allele for certain cases of CHD.

INTRODUCTION

Congenital heart disease (CHD) is a frequently occurring, developmental malformation and constitutes a high risk for infant mortality (Pierpont et al., 2007). It is characterized by abnormal development of the heart and its connected structures. Importantly, heart development is precisely controlled spatially as well as temporally. It starts long before the actual heart tube or its progenitor cells become evident. In particular the future heart's shape and placement relative to the other internal organs is determined by early left-right (LR) symmetry breaking in vertebrates (Ramsdell, 2005). At the cellular level, the most important structure for asymmetry is the temporal organ of laterality. It is a cup-like structure at the distal end of the notochord. Motile cilia within the temporal organ of laterality induce a flow by coordinated movement that triggers the expression of genes only on the left side of the

© 2013 The Authors. Published by Elsevier Inc. All rights reserved.

Corresponding author: Melanie Philipp, Ulm University, Department of Biochemistry and Molecular Biology, Fax: +49 731 500 23277, Phone: +49 731 500 23287, melanie.philipp@uni-ulm.de.

Publisher's Disclaimer: This is a PDF file of an unedited manuscript that has been accepted for publication. As a service to our customers we are providing this early version of the manuscript. The manuscript will undergo copyediting, typesetting, and review of the resulting proof before it is published in its final citable form. Please note that during the production process errors may be discovered which could affect the content, and all legal disclaimers that apply to the journal pertain.

body and thus internal asymmetry along the body axis (Essner et al., 2002; Okada et al., 2005; Oteiza et al., 2008). Not surprisingly, disturbances in the formation or function of the temporal organ of laterality interfere with proper heart development. This is reflected by the fact, that CHD is very common in individuals with irregular asymmetry establishment (Sutherland and Ware, 2009). This condition, where internal organs appear to find their placement randomly is known as isomerism, situs ambiguous or heterotaxy. The seriousness of the condition varies widely. While some patients experience complete rearrangement of internal organs such as in left or right isomerism, there can be cases, in which the heart occurs to be the only affected structure (i.e. dextrocardia).

The molecular causes underlying ciliary diseases and as such situs anomalies have been the focus of many studies in the past decade. Many signaling cascades were found to be of importance including basic morphogens such as Sonic hedgehog (Shh) or Bone morphogenetic protein 4 (Bmp4) (Schilling et al., 1999). In addition to those the mTOR pathway has emerged as a key pathway in ciliary physiology. Interestingly, mTOR activity appears to be controlled through bending of cilia. In kidney cells, loss of cilia or the movement thereof resulted in unrestricted mTOR signaling and cell growth (Boehlke et al., 2010). It thus has been implicated in the development of polycystic kidney disease (PKD) (Zullo et al., 2010), which belongs to the family of cilia-based diseases. In zebrafish, mTOR signaling could be linked to symmetry breaking. Deregulated mTOR activity within the organ of laterality or during the stages, when this organ is functional, has been shown to randomize lateralization (DiBella et al., 2009; Yuan et al., 2012).

GRK5 is one of seven kinases in vertebrates, which were named after their ability to terminate GPCR signal transduction (Premont and Gainetdinov, 2007). It is highly abundant in the heart with the effect that GRK5 is a major regulator of cardiac GPCRs and thus has a vital influence on heart physiology (Chen et al., 2001; Eckhart et al., 2000; Liggett et al., 2008; Martini et al., 2008; Rockman et al., 1996). Recent studies revealed that GRK5 modulates signal transduction also from non-GPCR receptors and even non-receptor proteins (Huang et al., 2011b). Together with its action on adrenoceptors (Chen et al., 2001; Rockman et al., 1996), it is thus capable of significantly altering cardiac physiology by interacting with molecules such as NF- κ B or histone deacetylases (Martini et al., 2008; Sorriento et al., 2010). These new functions are also promoted by GRK5's ability to act not only close to the cell membrane, but also in other subcellular localizations, such as the nucleus (Gold et al., 2012; Michal et al., 2012).

Interestingly, GRK5 is already expressed in the developing heart (Premont et al., 1999). We thus hypothesized that GRK5 may play an additional, yet unreported role in heart formation during early development, besides controlling proper heart physiology in the adult organism.

RESULTS and DISCUSSION

GRK5 facilitates cardiac looping

To investigate a potential role of GRK5 in the developing heart, we have used zebrafish as a model due to its advantages for developmental studies. We have applied a commonly used knockdown (KD) approach to generate GRK5 loss of function zebrafish embryos. Zebrafish have two genes located on two different chromosomes with homology to human GRK5. These homologs share little nucleotide sequence homology between one another. Multiple protein alignment analyses demonstrate that zebrafish Grk5l, encoded on chromosome 8, is the closer homolog to human GRK5 compared to zebrafish Grk5 on chromosome 10 (Figure S1A, B). Thus, a translation blocking antisense morpholino (MO) targeting the 5'-untranslated region (UTR) of Grk5l (Grk5l MO) was designed as well as a 5 bases mismatch control MO (CTRL MO). To confirm that the translation blocking MO targeting *grk5l*

sufficiently depletes Grk51, we co-injected capped mRNA encoding for a Grk51-GFP fusion protein, which was preceded by parts of *grk51*'s 5'-UTR. Embryos injected with Grk51 MO failed to produce GFP fluorescence (Figure 1A, A', A''). Moreover, KD efficiency was verified by Western blot (Figure S1C) and a MO binding assay (Figure S1D). Importantly, the 5'-UTRs of both *grk5* variants in zebrafish are not conserved and MOs targeting *grk51* are not predicted to bind to the UTR of *grk5*. We also did not find a feedback loop altering mRNA levels of *grk5* upon KD of Grk51 (Figure S1E) suggesting that any phenotype observed was likely due to specific KD of Grk51.

MO-mediated KD of Grk51 results initially in viable embryos which are morphologically very similar to non-injected WT (NI) embryos or embryos injected with the CTRL MO (Figure 1B, B', B''). After KD of Grk51, we allowed embryos to develop further and observed that Grk51 KD induces pericardiac edema and cardiac dilatation (Figure 1C to D). Two additional MOs targeting Grk51 either upstream of the first MO in the 5'-UTR or downstream around the start codon could validate this cardiac phenotype (Figure 1D and S1F). We thus examined Grk51 expression in the heart and observed *grk51* transcripts in cardiac tissue at 48 hours post fertilization (hpf) (Figure 1E). Furthermore, depletion of Grk51 affected also expression of genes in the heart, which were shown to be important for valve seeding (Figure 1F-K'). Chamber formation, however, occurred regularly (Figure 1L to M'). But importantly, hearts of Grk51 KD embryos injected with any of the three MOs either failed to loop or showed an inverse loop in roughly half of all embryos (Figure 1N, O), which might be attributed to failure in establishing LR asymmetry. KD of the single zebrafish homolog of GRK2 and GRK3, *Grk2/3*, displayed regular D-loops (Figure 1O). Interestingly, loss of the other *Grk5* in zebrafish resulted also in abnormal heart looping, although to a lesser extent. Combined KD of both, *Grk5* and *Grk51*, did not worsen the phenotype (Figure S1G, H). This implies that this function in early heart looping may be executed by both *grk5* genes. From these data we conclude that Grk51 influences heart development during its early formation.

Grk51 governs symmetry breaking

Morphological defects of cardiac structures in the context of looping irregularities are indicators of disrupted LR asymmetry development. Similarly, human heterotaxy patients, who suffer from random placement of thoracic and/or abdominal organs, often develop dextrocardia as well as valvular or septal defects (i.e. common single ventricle). Thus, frequent complications in heterotaxy patients include CHD. To test if Grk51 might govern proper cardiogenesis by ensuring asymmetry development, we analyzed genes which are expressed unilaterally at specific developmental stages (Sutherland and Ware, 2009). Using whole mount *in situ* hybridization (WMISH) at late somite stages (ss), we found that genes expressed in the left heart region, *bmp4* and the nodal target gene *lefty2*, are misexpressed upon Grk51 KD (Figure 2A, B). We next wondered, if Grk51's impact on lateralization could be seen earlier on the level of the lateral plate mesoderm (LPM), which also gives rise to the heart. The LPM-specific genes *southpaw* (*spaw*) and *pitx2* are ambiguously expressed in Grk51 morphants (Figure 2C, D). However, this false pattern can be partially rescued by co-injection of MO-insensitive synthetic *grk51*RNA (Figure 2C, D). Similarly, the correct distribution of *lefty2* could be rescued by *grk51*RNA (Figure 2B). Analysis of *lefty1* expression in the left diencephalon as well as pancreas placement in 2 days-post-fertilization (dpf) embryos demonstrated further that the lateralization defect upon loss of Grk51 is general (Figure 2E, F). Grk51 may therefore be a so far unanticipated gene involved in the determination of LR asymmetry.

Cilia length depends on Grk51

A prominent model in LR asymmetry development depends on the formation and function of cilia in the temporary organ of laterality (Kupffer's vesicle, KV, in zebrafish or the node in mice) (Sutherland and Ware, 2009). In line with this, zebrafish mutants for ciliary proteins often develop asymmetry defects, hydrocephalus and a distinct body curvature (Sun et al., 2004). Such curved body axis could also be observed upon depletion of Grk51 and was most prominent in embryos injected with MO3 (Figure S1F). We thus questioned whether Grk51 might act on or within the KV, especially since we found transcripts of *grk51*, which is expressed throughout development (Figure S2A–K), enriched in the tailbud region of embryos (Figure S2D–G).

First we tested, if the asymmetry defect was due to improper KV establishment. We analyzed midline formation as well as dorsal forerunner cell (DFC) clustering, both essential processes preceding KV differentiation (Bisgrove et al., 1999; Oteiza et al., 2008). Neither of those was altered upon Grk51 KD (Figure 3A). Additionally, the KV area was not changed (Figure 3B, C) indicating that Grk51 may potentially exert its function within the KV itself.

To test this, we targeted the MO to DFCs, which are the cells giving rise to the KV. This can be achieved by injection at the 1k cell stage. MO or RNA is then specifically delivered to DFCs and thus the KV (Amack and Yost, 2004). This chimeric KD of Grk51 was sufficient to interfere with proper heart looping as well as pancreas placement (Figure 3D, E). In addition we observed randomization of *spaw* expression (Figure 3F). We next wondered if Grk51 would localize to cilia. We detected Grk51 in primary cilia when expressed in NIH3T3 cells and in motile cilia in the pronephric duct (Figure 3G). We therefore investigated if Grk51 KD would affect cilia formation in zebrafish. Motile cilia of the developing pronephros were longer in Grk51 morphants compared to control embryos (Figure 3H, I). Those results suggested that a ciliary defect in the KV may possibly be the basis for the Grk51 phenotype. While we did not observe a significant change in cilia number (Figure 3J, K), we found cilia of Grk51-depleted KVs were significantly longer than in control injected embryos (Figure 3J, L). These findings are again in line with a common observation that zebrafish with ciliary deficiencies display a pronounced body curvature, which we had also observed (Figure S1F). These results suggest that Grk51 helps to regulate cilia formation in the developing embryo and by that ensures symmetry breaking.

Grk51 fine-tunes mTORC1 activity during symmetry breaking

We next wanted to identify the molecular mechanism causing the Grk51 KD phenotype. Overstimulation of β_{1b} -adrenoceptors (β_{1b} -AR) can cause lateralization defects (Fujinaga et al., 1994). As GRK5 attenuates elevated β_{1b} -AR signaling (Eckhart et al., 2000), we hypothesized that the observed phenotype could be caused by loss of Grk51-mediated β_{1b} -AR desensitization. However, WD-4101, an β_{1b} -AR specific inhibitor did not rescue situs inversus frequency in Grk51 KD embryos (Figure S3A). We thus wondered if the observed phenotype would potentially be due to Grk51 modulating signaling not at the GPCR level. However, no differences were found when we studied target gene expression of the Shh or retinoic acid signaling in Grk51 morphants (Figure S3B–D). Both pathways had been implicated in symmetry breaking before (Huang et al., 2011a; Schilling et al., 1999).

Previously, we have reported that Grk5 facilitates canonical Wnt signaling (Chen et al., 2009). As Grk51 might share this function, we tested its effect on *axin2* (Figure S3E). Grk51 appears to be a positive modulator of canonical Wnt signaling. Canonical Wnt signaling has also been reported to steer LR asymmetry development (Caron et al., 2012). However, impaired Wnt signaling is associated with shorter cilia, while we see elongated cilia. Grk51's

action on Wnt signaling may therefore not necessarily be related to its role in asymmetry development.

Recent studies on ciliary diseases including PKD and heterotaxy have highlighted the importance of the mammalian target of rapamycin complex 1 (mTORC1), which regulates cell growth (Zoncu et al., 2011). mTORC1 signaling has been connected to ciliary architecture and function and thus conditions which rely on cilia (Boehlke et al., 2010; DiBella et al., 2009; Yuan et al., 2012). We therefore investigated whether Grk5l influences mTORC1 activity by measuring phosphorylation of its target S6K1 in zebrafish embryos. We detected an increase in mTORC1 activity implicating a negative impact of Grk5l on mTORC1 activity (Figure 4A). This finding could be reproduced in hearts of young GRK5 knockout (KO) mice (Figure 4B). In addition, we found that transient overexpression of Grk5l in HEK293T cells caused a reduction of mTORC1 activity (Figure 4C) and a decrease in cell volume (Figure 4D). These results suggest that depletion of Grk5l might remove a dampening effect on mTORC1 activity and that an apparent mTORC1 overstimulation would be causal for the lateralization defect. To test this, we treated Grk5l KD embryos with the mTORC1 inhibitor rapamycin (rapa). Rapa rescued the lateralization phenotype of Grk5l KD embryos (Figure 4E and S4A), while control embryos were unaffected. Furthermore, a specific S6K1 inhibitor (Pearce et al., 2010; Rosner et al., 2012) could also rescue the phenotype (Figure 4F). We conclude from this that increased mTORC1 activity is causal for the asymmetry defects in the Grk5l KD embryos. To determine whether there may be a direct physical interaction, we performed co-immunoprecipitation assays in transfected as well as native cells. Raptor co-precipitated with overexpressed Grk5l (Figure 4G) as well as endogenous GRK5 (Figure S4B). Grk5l also co-localizes with the mTORC1 components mTOR, Raptor, and mLST8 in HEK293T cells (data not shown). These data are in line with our *in vivo* results and corroborate that Grk5l negatively regulates mTORC1 activity, probably through direct interaction with Raptor.

We also analyzed the spatial expression patterns of *grk5l* and *raptor* and found them to be very similar (Figure S2). Moreover, mRNA levels of both *grk5l* as well as *raptor* substantially increase at 10 hpf (Figure 4H, I), when the KV starts to form, the essential structure for symmetry breaking. We thus reasoned that a rescue of the Grk5l KD phenotype might also be achieved by inhibition of mTORC1 from 10 hpf on, which is what we observed (Figure S4A). Moreover, randomization of laterality could also be reversed by rapa, when Grk5l was knocked down specifically in the KV (Figure S4C). We conclude that Grk5l is needed to fine-tune mTORC1 activity at the level of the temporal organ of laterality in order to accomplish successful symmetry breaking.

Previously, it has always been assumed that GRK5 would be dispensable for embryonic development, primarily because GRK5 KO mice are viable (Gainetdinov et al., 1999). Yet, combined loss of GRK5 and GRK6 results in embryonic lethality (Table S1). A detailed characterization of this lethality remains to be undertaken and is subject of future studies in our lab.

In this study, we have used zebrafish to delineate the importance of vertebrate GRK5 during development. Similar to GRK5 KO mice, depletion of Grk5l in zebrafish does not necessarily result in embryonic lethality, but in a complex, often overlooked embryonic phenotype. Similarly, heterotaxy can have a plethora of mild phenotypes that are easily missed. Future studies will thus be required to illuminate if and how GRK5 would influence symmetry breaking in mammals.

In summary, we here provide evidence that vertebrate GRK5 possesses physiological relevance during development of the heart. We found that the close homolog in zebrafish,

Grk5l, is required to steer lateralization in zebrafish. By that it ensures proper cardiogenesis and may potentially prevent congenital heart defects, which are common complications in situs anomalies. Mechanistically, Grk5l confines mTORC1 signaling at the level of the temporal organ of asymmetry and controls ciliary morphology. Moreover, Grk5l potentially influences heart morphology by affecting expression of cardiac genes. The well-characterized role vertebrate GRK5 plays in the adult heart thus needs to be expanded to very early steps during development, when the body plan and thus a properly functioning heart is defined.

Experimental Procedures

Zebrafish and mouse experiments

Zebrafish were maintained under standard conditions at a 14 hours light and 10 hours dark cycle. Fertilized eggs were injected and allowed to develop at 28.5 °C. Mice lacking GRK5 and/or GRK6 were generated as described previously (Gainetdinov et al., 2003; Gainetdinov et al., 1999) and bred from heterozygous breeding pairs. Tissue for Western blotting was harvested from 3 to 5 months old animals. Housing of mice was under a 12 h light/dark cycle in a SPF facility. All husbandry and experiments described here were approved by German authorities or by the IACUC at Duke University. For further details regarding material and methods please refer to extended experimental procedures.

Supplementary Material

Refer to Web version on PubMed Central for supplementary material.

Acknowledgments

We thank the Zebrafish International Resource Center and many colleagues for providing reagents, Sabrina Matsyk for technical assistance, Cornelia Donow for help with the MO binding assay and Jim Burris and Julia Schäfer for fish maintenance. This work was supported in part by: FP7 of the European Commission (MP), Deutsche Stiftung für Herzforschung (MP), NIH grants NS-019576 and MH-073853 (MGC). During the initial stages of this work MP was the recipient of a Marie Curie Outgoing International Fellowship of the European Commission.

References

- Amack JD, Yost HJ. The T box transcription factor no tail in ciliated cells controls zebrafish left-right asymmetry. *Curr Biol.* 2004; 14:685–690. [PubMed: 15084283]
- Bisgrove BW, Essner JJ, Yost HJ. Regulation of midline development by antagonism of lefty and nodal signaling. *Development.* 1999; 126:3253–3262. [PubMed: 10375514]
- Boehlke C, Kotsis F, Patel V, Braeg S, Voelker H, Bredt S, Beyer T, Janusch H, Hamann C, Godel M, et al. Primary cilia regulate mTORC1 activity and cell size through Lkb1. *Nat Cell Biol.* 2010; 12:1115–1122. [PubMed: 20972424]
- Caron A, Xu X, Lin X. Wnt/beta-catenin signaling directly regulates Foxj1 expression and ciliogenesis in zebrafish Kupffer's vesicle. *Development.* 2012; 139:514–524. [PubMed: 22190638]
- Chen EP, Bittner HB, Akhter SA, Koch WJ, Davis RD. Myocardial function in hearts with transgenic overexpression of the G protein-coupled receptor kinase 5. *The Annals of thoracic surgery.* 2001; 71:1320–1324. [PubMed: 11308180]
- Chen M, Philipp M, Wang J, Premont RT, Garrison TR, Caron MG, Lefkowitz RJ, Chen W. G Protein-coupled receptor kinases phosphorylate LRP6 in the Wnt pathway. *J Biol Chem.* 2009; 284:35040–35048. [PubMed: 19801552]
- DiBella LM, Park A, Sun Z. Zebrafish Tsc1 reveals functional interactions between the cilium and the TOR pathway. *Hum Mol Genet.* 2009; 18:595–606. [PubMed: 19008302]

- Eckhart AD, Duncan SJ, Penn RB, Benovic JL, Lefkowitz RJ, Koch WJ. Hybrid transgenic mice reveal in vivo specificity of G protein-coupled receptor kinases in the heart. *Circ Res.* 2000; 86:43–50. [PubMed: 10625304]
- Essner JJ, Vogan KJ, Wagner MK, Tabin CJ, Yost HJ, Brueckner M. Conserved function for embryonic nodal cilia. *Nature.* 2002; 418:37–38. [PubMed: 12097899]
- Fujinaga M, Hoffman BB, Baden JM. Receptor subtype and intracellular signal transduction pathway associated with situs inversus induced by alpha 1 adrenergic stimulation in rat embryos. *Dev Biol.* 1994; 162:558–567. [PubMed: 8150214]
- Gainetdinov RR, Bohn LM, Sotnikova TD, Cyr M, Laakso A, Macrae AD, Torres GE, Kim KM, Lefkowitz RJ, Caron MG, et al. Dopaminergic supersensitivity in G protein-coupled receptor kinase 6-deficient mice. *Neuron.* 2003; 38:291–303. [PubMed: 12718862]
- Gainetdinov RR, Bohn LM, Walker JK, Laporte SA, Macrae AD, Caron MG, Lefkowitz RJ, Premont RT. Muscarinic supersensitivity and impaired receptor desensitization in G protein-coupled receptor kinase 5-deficient mice. *Neuron.* 1999; 24:1029–1036. [PubMed: 10624964]
- Gold JI, Gao E, Shang X, Premont RT, Koch WJ. Determining the absolute requirement of g protein-coupled receptor kinase 5 for pathological cardiac hypertrophy: short communication. *Circ Res.* 2012; 111:1048–1053. [PubMed: 22859683]
- Huang S, Ma J, Liu X, Zhang Y, Luo L. Retinoic acid signaling sequentially controls visceral and heart laterality in zebrafish. *J Biol Chem.* 2011a; 286:28533–28543. [PubMed: 21669875]
- Huang ZM, Gold JI, Koch WJ. G protein-coupled receptor kinases in normal and failing myocardium. *Frontiers in bioscience : a journal and virtual library.* 2011b; 17:3047–3060.
- Jaffe KM, Thiberge SY, Bisher ME, Burdine RD. Imaging cilia in zebrafish. *Methods Cell Biol.* 2010; 97:415–435. [PubMed: 20719283]
- Liggett SB, Cresci S, Kelly RJ, Syed FM, Matkovich SJ, Hahn HS, Diwan A, Martini JS, Sparks L, Parekh RR, et al. A GRK5 polymorphism that inhibits beta-adrenergic receptor signaling is protective in heart failure. *Nat Med.* 2008; 14:510–517. [PubMed: 18425130]
- Martini JS, Raake P, Vinge LE, DeGeorge BR Jr, Chuprun JK, Harris DM, Gao E, Eckhart AD, Pitcher JA, Koch WJ. Uncovering G protein-coupled receptor kinase-5 as a histone deacetylase kinase in the nucleus of cardiomyocytes. *Proc Natl Acad Sci U S A.* 2008; 105:12457–12462. [PubMed: 18711143]
- Michal AM, So CH, Beeharry N, Shankar H, Mashayekhi R, Yen TJ, Benovic JL. G Protein-coupled receptor kinase 5 is localized to centrosomes and regulates cell cycle progression. *J Biol Chem.* 2012; 287:6928–6940. [PubMed: 22223642]
- Okada Y, Takeda S, Tanaka Y, Belmonte JC, Hirokawa N. Mechanism of nodal flow: a conserved symmetry breaking event in left-right axis determination. *Cell.* 2005; 121:633–644. [PubMed: 15907475]
- Oteiza P, Koppen M, Concha ML, Heisenberg CP. Origin and shaping of the laterality organ in zebrafish. *Development.* 2008; 135:2807–2813. [PubMed: 18635607]
- Pearce LR, Alton GR, Richter DT, Kath JC, Lingardo L, Chapman J, Hwang C, Alessi DR. Characterization of PF-4708671, a novel and highly specific inhibitor of p70 ribosomal S6 kinase (S6K1). *Biochem J.* 2010; 431:245–255. [PubMed: 20704563]
- Philipp M, Fralish GB, Meloni AR, Chen W, MacInnes AW, Barak LS, Caron MG. Smoothed signaling in vertebrates is facilitated by a G protein-coupled receptor kinase. *Mol Biol Cell.* 2008; 19:5478–5489. [PubMed: 18815277]
- Pierpont ME, Basson CT, Benson DW Jr, Gelb BD, Giglia TM, Goldmuntz E, McGee G, Sable CA, Srivastava D, Webb CL. Genetic basis for congenital heart defects: current knowledge: a scientific statement from the American Heart Association Congenital Cardiac Defects Committee, Council on Cardiovascular Disease in the Young: endorsed by the American Academy of Pediatrics. *Circulation.* 2007; 115:3015–3038. [PubMed: 17519398]
- Premont RT, Gainetdinov RR. Physiological roles of G protein-coupled receptor kinases and arrestins. *Annual review of physiology.* 2007; 69:511–534.
- Premont RT, Macrae AD, Aparicio SA, Kendall HE, Welch JE, Lefkowitz RJ. The GRK4 subfamily of G protein-coupled receptor kinases. Alternative splicing, gene organization, and sequence conservation. *J Biol Chem.* 1999; 274:29381–29389. [PubMed: 10506199]

- Ramsdell AF. Left-right asymmetry and congenital cardiac defects: getting to the heart of the matter in vertebrate left-right axis determination. *Dev Biol.* 2005; 288:1–20. [PubMed: 16289136]
- Rockman HA, Choi DJ, Rahman NU, Akhter SA, Lefkowitz RJ, Koch WJ. Receptor-specific in vivo desensitization by the G protein-coupled receptor kinase-5 in transgenic mice. *Proc Natl Acad Sci U S A.* 1996; 93:9954–9959. [PubMed: 8790438]
- Rosner M, Schipany K, Hengstschlager M. p70 S6K1 nuclear localization depends on its mTOR-mediated phosphorylation at T389, but not on its kinase activity towards S6. *Amino Acids.* 2012; 42:2251–2256. [PubMed: 21710263]
- Schilling TF, Concordet JP, Ingham PW. Regulation of left-right asymmetries in the zebrafish by Shh and BMP4. *Dev Biol.* 1999; 210:277–287. [PubMed: 10357891]
- Sorriento D, Santulli G, Fusco A, Anastasio A, Trimarco B, Iaccarino G. Intracardiac injection of AdGRK5-NT reduces left ventricular hypertrophy by inhibiting NF-kappaB-dependent hypertrophic gene expression. *Hypertension.* 2010; 56:696–704. [PubMed: 20660817]
- Sun Z, Amsterdam A, Pazour GJ, Cole DG, Miller MS, Hopkins N. A genetic screen in zebrafish identifies cilia genes as a principal cause of cystic kidney. *Development.* 2004; 131:4085–4093. [PubMed: 15269167]
- Sutherland MJ, Ware SM. Disorders of left-right asymmetry: heterotaxy and situs inversus. *American journal of medical genetics Part C, Seminars in medical genetics.* 2009; 151C:307–317.
- Yuan S, Li J, Diener DR, Choma MA, Rosenbaum JL, Sun Z. Target-of-rapamycin complex 1 (Torc1) signaling modulates cilia size and function through protein synthesis regulation. *Proc Natl Acad Sci U S A.* 2012; 109:2021–2026. [PubMed: 22308353]
- Zoncu R, Efeyan A, Sabatini DM. mTOR: from growth signal integration to cancer, diabetes and ageing. *Nat Rev Mol Cell Biol.* 2011; 12:21–35. [PubMed: 21157483]
- Zullo A, Iaconis D, Barra A, Cantone A, Messaddeq N, Capasso G, Dolle P, Igarashi P, Franco B. Kidney-specific inactivation of *Ofd1* leads to renal cystic disease associated with upregulation of the mTOR pathway. *Hum Mol Genet.* 2010; 19:2792–2803. [PubMed: 20444807]

Highlights

GRK5 has a role during early embryonic development by guiding symmetry breaking.

GRK5 modulates cilia length in the organ of laterality by negatively regulating mTOR.

GRK5 regulates heart development.

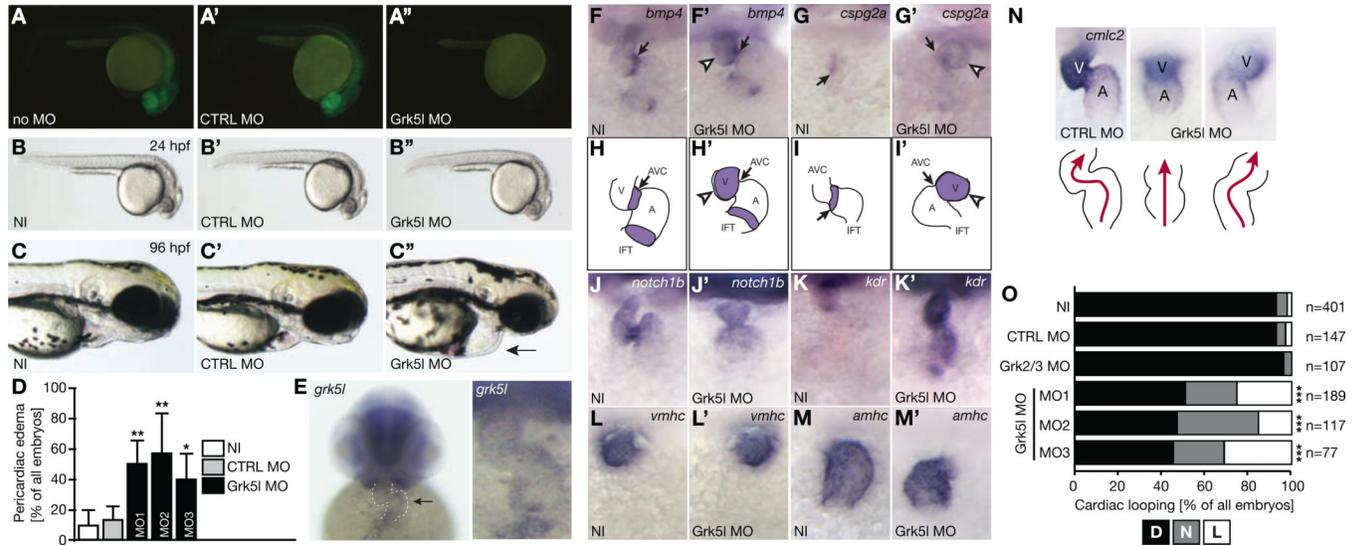


Figure 1. Grk51 KD in zebrafish affects early heart development

A, A', A'', Grk51 MO prevents translation of co-injected RNA coding for Grk51-GFP fused to parts of its 5'-UTR and results in fish showing no glowing (A''), while RNA injection alone (A) or in combination with the CTRL MO (A') produces strong GFP expression.

B, B', B'', 24 hpf zebrafish embryos injected with Grk51 MO (B'') compared to non-injected embryos (NI) (B) or those injected with CTRL MO (B').

C, C', C'', Live embryos (96 hpf). Arrow indicates pericardial edema in Grk51 morphants.

D, Bar graph displaying the percentage of embryos with pericardial edema. $n=3-10$ experiments, 76 to 340 embryos. CTRL MO vs. Grk51 MO: $p=0.0023$; CTRL MO vs. Grk51 MO2: $p=0.0016$, CTRL MO vs. Grk51 MO3: $p=0.0213$.

E, *grk51* transcripts in the heart of 48 hpf zebrafish embryos (arrow and higher magnification).

F, F', *Bmp4* transcripts are upregulated and dispersed throughout the heart of Grk51 morphants (F'). $n=10-35$.

G, G', Upregulation of *cspg2a* upon injection of Grk51 MO (G'). $n=16-18$.

H, H', Illustration of normal distribution of *bmp4* in controls (H) and widespread expression in Grk51 morphants (H').

I, I', Cartoon showing the regular as well as aberrant distribution of *cspg2a* in controls (I) and Grk51 MO (I') injected fish.

J, J', *Notch1b* fails to accumulate in the future valve region upon Grk51 KD (J'). $n=16-25$.

K, K', *Kdr* is strongly upregulated upon KD of Grk51 (K') compared to control fish (K). $n=5-22$.

L, L', Ventricular fate as shown by WMISH for *vmhc* is properly established when Grk51 is lost. $n=27-32$.

M, M', *Amhc* expression in the atrium. $n=18-23$.

N, WMISH for *cmlc2* at 50 hpf revealing altered cardiac looping in Grk51 morphants (arrow). Cartoon depicts heart morphology and blood flow. A, atrium, V, ventricle.

O, Summary of heart looping after injection with MOs targeting either Grk2/3 or Grk51. For Grk51, three different MOs were tested. D, D-loop, N, no loop, L, L-loop. CTRL MO vs. Grk51 MO: $p<0.0001$; CTRL MO vs. Grk51 MO2: $p<0.0001$; CTRL MO vs. Grk51 MO3: $p<0.0001$.

F to M: All images: 48 to 52 hpf.
See also Figure S1 and Table S1.

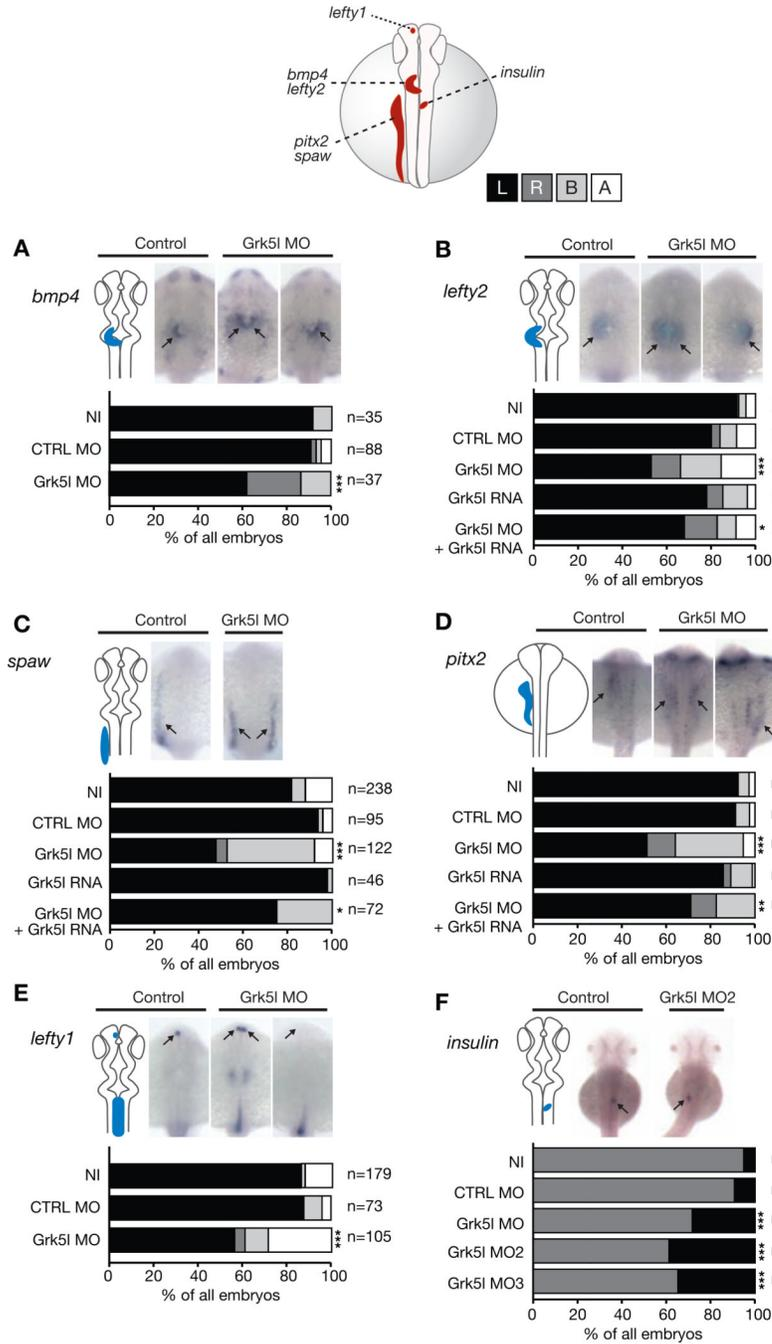


Figure 2. Grk51 governs LR asymmetry development

WMISH for leftward marker genes at 20–22 ss with the respective expression domain outlined next to the images. Bar graphs display percentages of expression on the left side (black), on the right (dark grey), on both sides of the midline (light grey) or no expression at all (white).

A, *bmp4* expression in the heart region is randomized upon Grk51 KD. CTRL MO vs Grk51 MO: $p=0.0056$.

B, Random distribution of *lefty2* can be partially rescued by *grk51* RNA. CTRL MO vs Grk51 MO: $p<0.0001$; Grk51 MO vs Grk51 MO+*grk51* RNA: $p=0.0425$.

C, *spaw* in the LPM is affected upon loss of Grk51, but can be rescued by co-injection of *grk51* mRNA. CTRL MO vs Grk51 MO: $p < 0.0001$; Grk51 MO vs Grk51 MO+*grk51*RNA: $p = 0.0002$.

D, Ambiguous *pitx2* reversed by mRNA encoding for *grk51*. CTRL MO vs Grk51 MO: $p < 0.0001$; Grk51 MO vs Grk51 MO+*grk51*RNA: $p = 0.0068$.

E, *Lefty1* transcripts in the dorsal diencephalon are ambiguously distributed, when Grk51 is lost. CTRL MO vs Grk51 MO: $p < 0.0001$.

F, Loss of Grk51 interferes with pancreas placement, as can be seen by the expression of *insulin*. CTRL MO vs Grk51 MO: $p = 0.0009$; CTRL MO vs Grk51 MO2: $p < 0.0001$; CTRL MO vs Grk51 MO3: $p < 0.0001$.

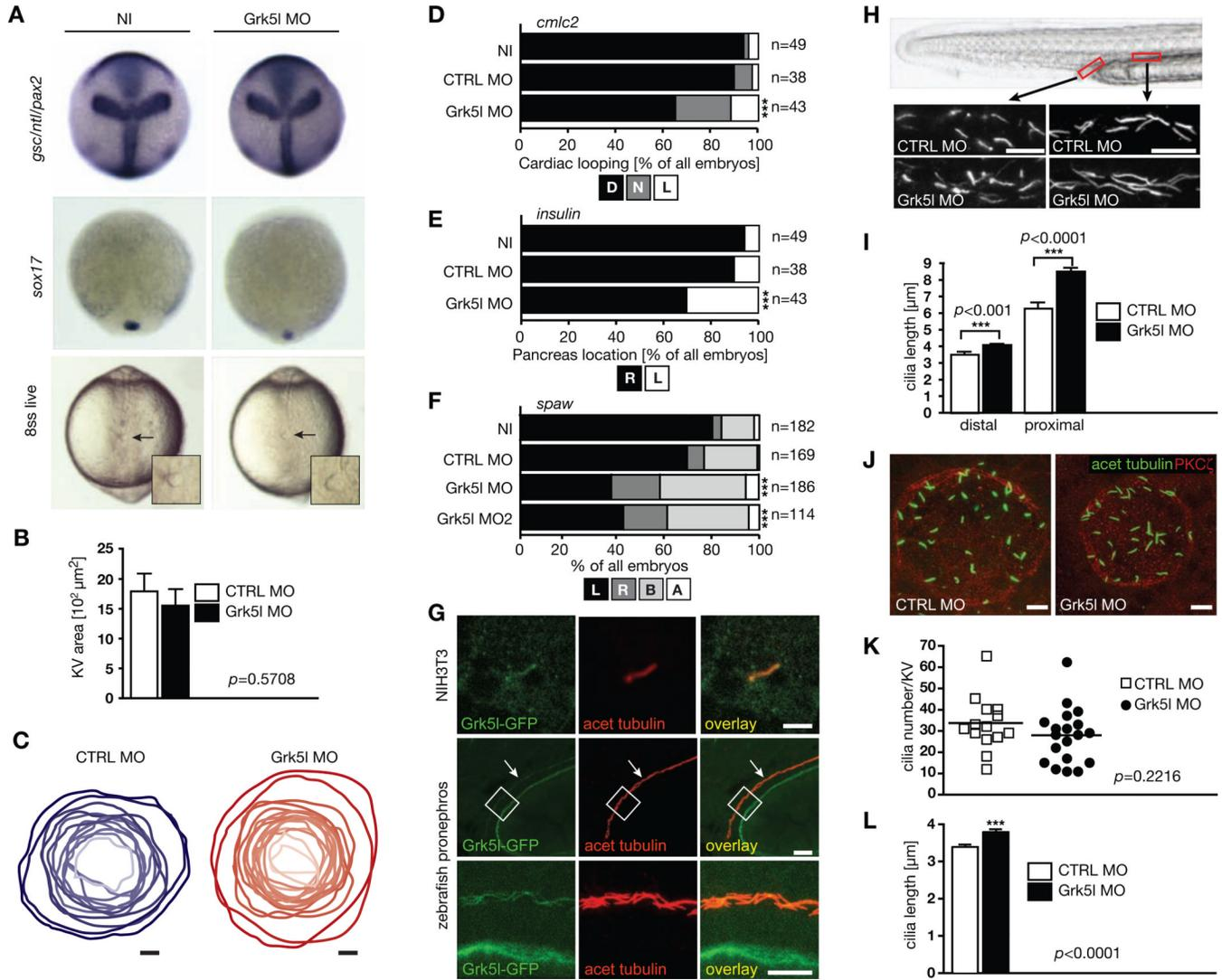


Figure 3. Grk51 acts in the organ of laterality

A, Combined WMISH for *gsc*, *ntl* and *pax2* (10hpf). DFCs cluster normally at 90% epiboly as shown by *sox17* (n=32–35). Live imaging at 8 ss shows that the KV forms. Arrows indicate KV, higher magnification in inset.

B, KV-specific KD did not alter KV area as assessed by PKC staining at 8 ss. n=14–19 embryos. CTRL MO: $1793 \pm 299 \mu\text{m}^2$, Grk51 MO: $1555 \pm 277 \mu\text{m}^2$.

C, Outline of KVs upon injection of CTRL MO (blue) or of Grk51 MO (red). Dependent on the respective size, the KV is shown in darker or brighter shading. n=12–17 embryos.

D, Impaired heart looping by Grk51 depletion in KV cells detected by *cmhc2* ISH at 50 hpf. CTRL MO vs Grk51 MO: $p<0.0001$.

E, *Insulin*-positive cells of the pancreas are more often on the left side of the midline upon KV-specific KD of Grk51. CTRL MO vs Grk51 MO: $p=0.0007$.

F, KV-directed ablation of Grk51 randomizes *spaw*. CTRL MO vs Grk51 MO: $p<0.0001$; CTRL MO vs Grk51 MO2: $p=0.0002$.

G, Grk51 localizes to primary cilia in NIH3T3 cells and motile cilia in the developing zebrafish kidney. Images show Grk51-GFP after transfection in cells or injection of capped RNA into 1 cell stage embryos. Scale bars: 3 μm (NIH3T3), 20 μm (low magnification of pronephros), 10 μm (higher magnification).

H, Elongation of motile cilia of the zebrafish pronephros (2 dpf). Cilia in the distal (CTRL MO: $3.571 \pm 0.116 \mu\text{m}$, Grk51 MO: $4.090 \pm 0.0852 \mu\text{m}$) and proximal part (CTRL MO: $6.347 \pm 0.318 \mu\text{m}$, Grk51 MO: $8.526 \pm 0.220 \mu\text{m}$) were analyzed. Approximate areas of analysis are indicated in red in the live image of a 2 dpf zebrafish tail. Scale bar: $10 \mu\text{m}$.

I, Bar graph summarizing pronephric cilia measurements (n=32–101 cilia).

J, Motile cilia at 8 ss with MOs targeted to KV cells. Images were selected for cilia length. Scale bar: $10 \mu\text{m}$.

K, Cilia number was not altered in the KV by MOs targeted to the KV (8 ss). n=14–19 embryos. CTRL MO: 34.14 ± 3.372 cilia; Grk51 MO: 28.53 ± 2.960 cilia.

L, Grk51 depletion in the KV increases cilia length. n=460–513 cilia at 8 ss. CTRL MO: $3.344 \pm 0.049 \mu\text{m}$; Grk51 MO: $3.748 \pm 0.054 \mu\text{m}$.; $p < 0.0001$, two-tailed, unpaired t-test. See also Figure S3.

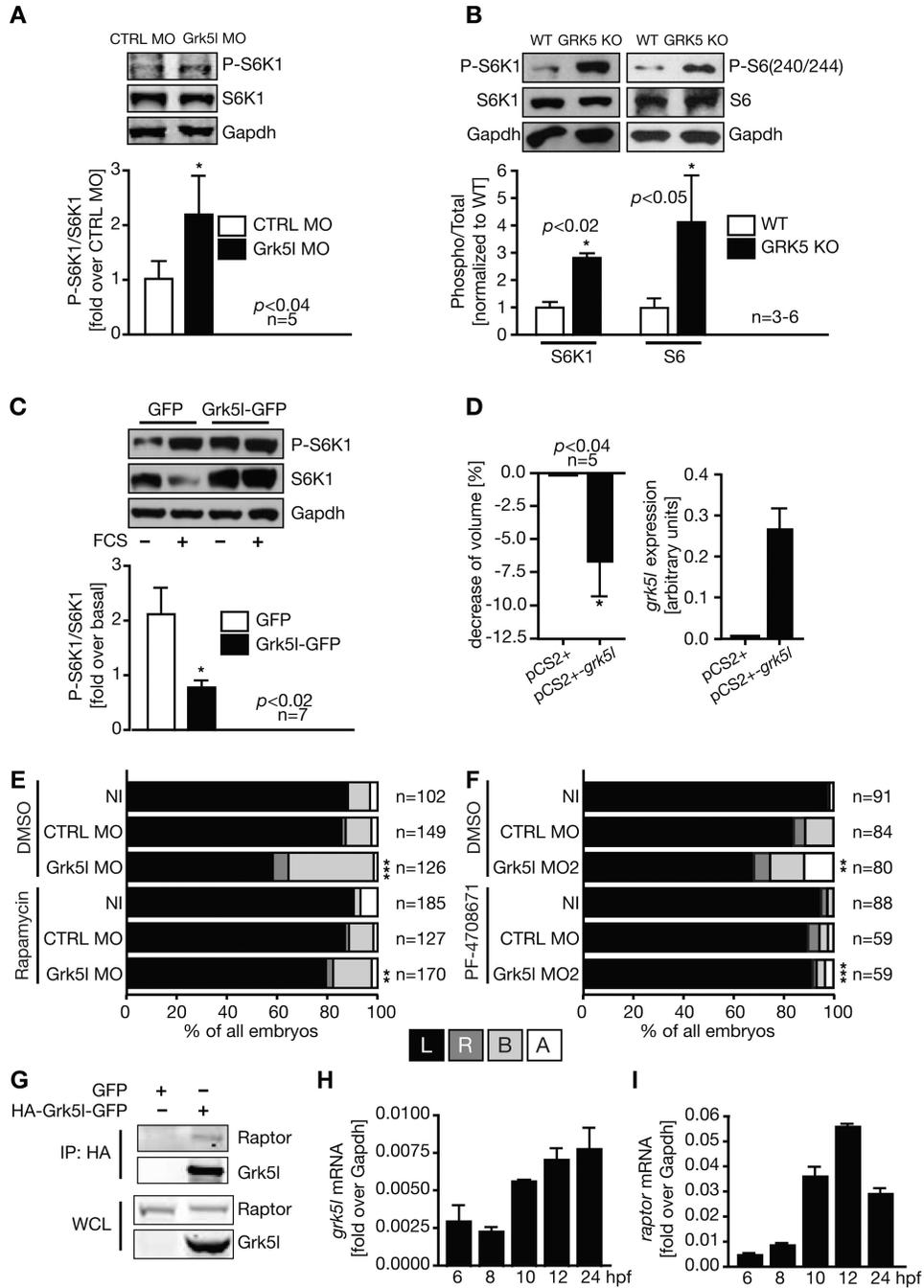


Figure 4. Grk51 limits mTOR signaling

A, Western blot analysis of zebrafish embryos (6–8 ss) for S6K1 phosphorylation. Representative images of a single blot shown.

B, Western blot of mouse heart lysates of wild-type (WT) and GRK5 KO mice for phosphorylation of S6K1 and its target ribosomal protein S6.

C, Overexpression of Grk51-GFP in cells attenuates TORC1 activity towards S6K1.

D, Cell volume of Grk51 transfected cells (left, mean \pm SEM). Cells were controlled for *grk5l* expression (right graph, means \pm SD, $n = 2-3$).

E, Reversal of the Grk51 lateralization phenotype by rapa. Analysis of *spaw* in the presence of DMSO or rapa from 6 to 10 hpf. CTRL MO^{DMSO} vs Grk51 MO^{DMSO}: $p < 0.0001$; Grk51 MO^{DMSO} vs Grk51 MO^{Rapa}: $p = 0.0033$.

F, Inhibition of S6K1 activity by PF-470871 reverses the *spaw* misexpression upon Grk51 KD. CTRL MO^{DMSO} vs Grk51 MO^{2DMSO}: $p = 0.0063$; Grk51 MO^{2DMSO} vs Grk51 MO^{2PF}: $p < 0.0001$.

G, Co-immunoprecipitation of transfected GFP or HA- Grk51-GFP and endogenous Raptor using a HA-antibody. IP, immunoprecipitation; WCL, whole cell lysate.

H, Relative expression levels of *grk51* obtained by qPCR (mean \pm SD, $n = 2$).

I, *raptor* mRNA levels (mean \pm SD, $n = 2$).

See also Figures S2, S3, and S4.